# A Model Predictive Control based Power Sharing Control of Dual Active Bridge Converter with Parameters Estimation

Li, Yuan; Sahoo, Subham; Dragičević, Tomislav; Zhang, Yichao; Blaabjerg, Frede

*Published in:*
Proceedings of the IECON 2022 – 48th Annual Conference of the IEEE Industrial Electronics Society

*DOI (link to publication from Publisher):*
10.1109/IECON49645.2022.9968713

*Publication date:*
2022

*Document Version*
Accepted author manuscript, peer reviewed version

# A Model Predictive Control based Power Sharing Control of Dual Active Bridge Converter with Parameters Estimation

Yuan Li
AAU Energy
Aalborg University
Aalborg, Denmark
e-mail: yuanli@energy.aau.dk

Subham Sahoo
AAU Energy
Aalborg University
Aalborg, Denmark
e-mail: sssa@energy.aau.dk

Tomislav Dragičević
Department of Electrical Engineering
Technical University of Denmark
Copenhagen, Denmark
e-mail: tomdr@elektro.dtu.dk

Yichao Zhang
AAU Energy
Aalborg University
Aalborg, Denmark
e-mail: yzha@energy.aau.dk

Frede Blaabjerg
AAU Energy
Aalborg University
Aalborg, Denmark
e-mail: fbl@energy.aau.dk

***Abstract*—Dual active bridge (DAB) converters are becoming one of the most reliable interfaces due to their high voltage range, easy realization of zero voltage switching (ZVS), galvanic isolation, etc. To meet specific consumer requirements in DC microgrids, DAB converters operate with different topologies. In this paper, a finite control set model predictive control (FCS-MPC)-based power sharing control is proposed when DAB converters are in different structures which are input series-output series, input parallel-output parallel, input parallel-output series, and input parallel-output parallel connecting structures. By analyzing the power balance relationship of the input port and output port, it determines the variable (input voltage/current or output voltage/current) which should be controlled to realize the power sharing. And then the cost function is designed based on the control strategy. Besides, this paper proposes a Kalman filter based parameter estimation method for the DAB converter. In this case, it guarantees the robustness of the MPC algorithm. Finally, the simulation results prove the effectiveness of the proposed method.**

***Keywords*—DAB converter; power sharing; model predictive control; parameters estimation; Kalman filter.**

## I. Introduction

In recent years, dual active bridge (DAB) converters with a guaranteed and reliable operation are widely used in DC microgrids [1]-[4]. When DAB modules are connected in the DC microgrid with electronic loads, they behave as the point of load converters. And these converters could perform as constant power loads (CPLs). Conventional stabilization solutions employ PI controllers to compensate for the impedance according to the impedance-based approach [5]-[6]. However, this kind of approach will bring degradation to the load regulation performance and lead to possible saturation of the original PI controller. Recently, model predictive control (MPC) is proved to be with advantage in solving the stabilization issue [7]. One of its merits is easy to describe the control targets in the cost function. Utilizing this characteristic, the input and output voltage damping have been integrated into the cost function to ensure stability [8]-[9].

To meet specific requirements, the DAB modules' structures can be divided into four types [10]. The first structure is called the input series and output series connected (ISOS) DAB system. This kind of system is applied to a situation that needs large input and output currents. Similarly, an input-series, output-parallel (ISOP) system is usually applied when a large input current and a large output voltage are required. Input-parallel, output-series (IPOS) structure is suitable when large input voltage and large output current are demanded. Lastly, an input-parallel and output-parallel (IPOP) structure is used in the system, which needs a large input current as well as a large output current.

For the discussed structures, the key issue arises when the power needs to be shared among each module. In [11], it proposes an output voltage sharing control for ISOS systems based on the master-slave control. It selects one module as the master controller and the other modules' controller will generate the control signal based on the master controller. In [12], a duty exchanging control for sharing the output voltage is proposed by adopting the averaged duty cycle of other modules. An input voltage sharing algorithm is proposed for ISOP systems based on master-slave control by introducing the average input voltage value as the reference in the control loop [13]. Similarly, an output current sharing control for ISOP systems is proposed by introducing the average value of other modules into the control loop [14]. For IPOS systems, an output voltage sharing algorithm is proposed based on master-slave control [15]. Independent control for output voltage sharing by directly introducing equal output voltage reference to each control loop is proposed [16]. For IPOP systems, the control for output current sharing is proposed with master-slave control or average current control [17]-[18]. However, the above control methods which are based on the master-slave controller will lead to low reliability. If the master module collapses, the system will be severely influenced. Although the average voltage/current control strategy can operate without a master-slave control format, it

This work was supported by the State Scholarship Fund of China Scholarship Council (CSC).

needs several sensors in the systems to measure the voltage/current for each control loop.

Combining the above stability and power sharing issues for DAB modules in the DC microgrid, the MPC algorithm is a reliable candidate. To improve the power balance control algorithm, a PI and MPC composed algorithm is proposed [14] for output current sharing with IPOP DAB converters, which shows an excellent sharing performance and high reliability as well as fewer sensors. However, other structures with the MPC algorithm have few related studies.

Although MPC is proved to be efficient and easy to contain constraints, it relies on the system model to establish control. During the operation, the parameters are not possible to remain at a constant value. Hence, to guarantee robustness, the estimation of the parameter's changes is crucial and necessary for MPC controlled system. Besides, the parameters' estimation is also widely used in the condition monitoring occasion [20]. In [17], it proposes a parameter estimation algorithm by introducing the perturbation into the control signal. According to the control signal's incremental or decremental value, it can estimate the parameters for each module. A leakage inductance estimation method based on the recursive least square (RLS) algorithm is proposed for an MPC-controlled single DAB converter [21]. Compared with the RLS estimation algorithm, a self-tuned Kalman filter estimation algorithm based on the system's transfer function is proved to show better estimation accuracy [22]. Nevertheless, because of the strong non-linear characteristics of an MPC controlled system, the system transfer function cannot be obtained easily and accurately, which will then severely affect the estimation accuracy.

To address the above issues, this paper proposes the power sharing strategies for the above four structures of DAB converters using the MPC algorithm. Moreover, this paper proposes a Kalman filter-based parameters estimation method for the DAB converter. The rest of the paper is organized as follows. Section II describes the studied DAB converter and proposes the power sharing control algorithm. Section III introduces the operating principle of the Kalman filter and proposes a Kalman filter-based parameters estimation algorithm for an MPC-controlled DAB converter. Section IV presents the simulation results. And Section V concludes the paper.

## II. Model Predictive Control of the Dual Active Bridge Converter

### A. Modeling of DAB converters with FCS-MPC

The DC-DC DAB converter is shown in Fig. 1. Generally, the input *LC* filter is supplemented before the input port of the DAB converter to provide a smooth input.

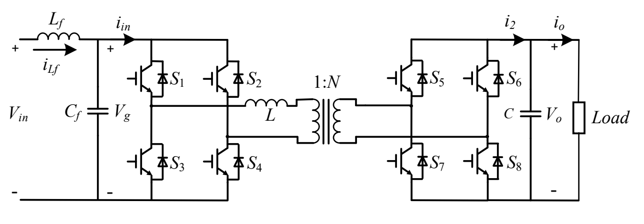


Fig. 1. DC-DC DAB converter.

The primary side of the DAB converter consists of four switches, which are $S_1$ to $S_4$, and with the primary side of the transformer. In this paper, the leakage inductance $L$ is considered on the primary side. The secondary side of the DAB converter consists of four switches, which are $S_5$ to $S_8$, and with the secondary side of the transformer. $N$ is the transformer ratio. $V_g$ and $V_o$ represent the input voltage and output voltage respectively.

The phase shift control is a common approach for controlling the DC-DC DAB converter. In this study, the single-phase shift approach is adopted. The control variable is defined as $\varphi$, which represents the phase shift between the primary side signal for $S_1$ and the secondary side signal for $S_5$. And the duty cycles of these eight switches are fixed at 0.5.

It can be seen that the DAB converter transforms the power through the intermediate transformer. According to the reduced-order model [14] for the DAB converter, the average power flows from the input to output is defined as:

$$P = \frac{V_g V_o}{2NL}\varphi(1-2\varphi) \tag{1}$$

where $P$ represents the output power of the load. From the studied system in Fig. 1, the following equations can be obtained:

$$\begin{cases} \dfrac{dV_g}{dt} = \dfrac{i_{Lf} - i_{in}}{C_f} \\ \dfrac{dV_o}{dt} = \dfrac{i_2 - \dfrac{P}{V_o}}{C} \end{cases} \tag{2}$$

Substituting (1) into (2), the following equation can be obtained:

$$\begin{cases} \dfrac{dV_g}{dt} = \dfrac{i_{Lf} - \dfrac{V_o}{2NL}\varphi(1-2\varphi)}{C_1} \\ \dfrac{dV_o}{dt} = \dfrac{\dfrac{V_g}{2NL}\varphi(1-2\varphi) - \dfrac{P}{V_o}}{C} \end{cases} \tag{3}$$

Assuming that the sampling frequency is relatively high, the state in (3) can be transformed into a discrete-time equation with the classical forward Euler approximation method. It is expressed as:

$$\begin{cases} \dfrac{dV_g}{dt} = \dfrac{V_g(k+1) - V_g(k)}{T_s} \\ \dfrac{dV_o}{dt} = \dfrac{V_o(k+1) - V_o(k)}{T_s} \end{cases} \tag{4}$$

where $T_s$ is the switching period. Combining the above equations, the predicted input voltage, and the capacitor voltage at the next sampling time $k$+1 can be expressed as:

$$\begin{cases} V_g(k+1) = V_g(k) + \dfrac{i_{Lf}(k) - \dfrac{V_o(k)}{2NL}\varphi(k)(1-2\varphi(k))}{C_f} T_s \\ V_o(k+1) = V_o(k) + \dfrac{\dfrac{V_g(k)}{2NL}\varphi(k)(1-2\varphi(k)) - \dfrac{P}{V_o(k)}}{C} T_s \end{cases} \tag{5}$$

The above equation is defined as the prediction model for the FCS-MPC algorithm. According to (5), the cost function is expressed as:

$$J=\sum_{l=1}^{N_h}(V_g(k+l)-V_g^*)^2+(V_o(k+1)-V_o^*)^2 \tag{6}$$

where, $N_h$ is the prediction horizon and $V_g^*$ and $V_o^*$ are the desired references. Finally, a control signal $\varphi$, which is the optimal shifting phase is selected and applied to the converter by minimizing the cost function in (6).

*B. Power sharing strategy of Multi DAB converters with FCS-MPC*

The structures of the connections between two DAB converters can be divided into four main groups shown in Fig. 2.

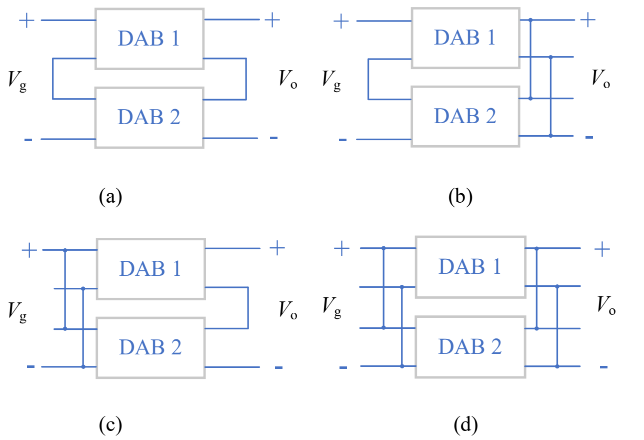


Fig. 2. Different structures of DAB converters. (a) ISOS. (b) ISOP. (c) IPOS. (d) IPOP.

Considering the power balancing issue in the above four structures, they can be classified into two different conditions, which are the voltage-controlled power sharing method and the current-controlled power sharing method.

Assuming minimal power loss between the transformation from the input port to the output port, we can get:

$$N_n V_g i_{in}=N_n V_o i_o \tag{7}$$

where $N_n$ is the number of DAB converters series or parallel connected. The objective for realizing the power balance can be expressed as:

$$\begin{cases}V_{g1}=V_{g2}=V_{g3}=\ldots=V_{gNn}\\ i_{in1}=i_{in2}=i_{in3}=\ldots=i_{inNn}\\ i_{o1}=i_{o2}=i_{o3}=\ldots=i_{oNn}\end{cases}$$
$$or \tag{8}$$
$$\begin{cases}V_{o1}=V_{o2}=V_{o3}=\ldots=V_{oNn}\\ i_{o1}=i_{o2}=i_{o3}=\ldots=i_{oNn}\\ i_{in1}=i_{in2}=i_{in3}=\ldots=i_{inNn}\end{cases}$$

Next, the power balance realization with these four structures based on FCS-MPC will be analyzed.

Firstly, the ISOS DAB converters are analyzed. According to the structure, it is intuitive that the DAB converters satisfy the equation as:

$$\begin{cases}i_{in1}=i_{in2}=i_{in3}=\ldots=i_{inNn}\\ i_{o1}=i_{o2}=i_{o3}=\ldots=i_{oNn}\end{cases} \tag{9}$$

Thus, the realization of power sharing is to make the output voltage of each DAB converter equal to $V_{ot}/N_n$, where $V_{ot}$ is the total output voltage of the multi-DAB converters. Hence, the control strategy can be expressed with FCS-MPC as:

$$J=\sum_{l=1}^{N_h}(V_{oi}(k+1)-V_o^*)^2 \qquad V_o^*=\frac{V_{ot}}{N_n} \tag{10}$$

where $i$=1, 2… $N_n$. Similarly, the ISOP DAB converters satisfy the equation:

$$\begin{cases}i_{in1}=i_{in2}=i_{in3}=\ldots=i_{inNn}\\ V_{o1}=V_{o2}=V_{o3}=\ldots=V_{oNn}\end{cases} \tag{11}$$

Thus, the realization of power sharing is to make the input voltage of each DAB converter equal to $V_g/N_n$, where $V_g$ is the total output voltage of the multi-DAB converters. Hence, the control strategy should be expressed with FCS-MPC as:

$$J=\sum_{l=1}^{N_h}[(V_{gi}(k+l)-V_g^*)^2+(V_{oi}(k+l)-V_o^*)] \qquad V_g^*=\frac{V_{gt}}{N_n} \qquad V_o^*=V_{ot} \tag{12}$$

When the IPOS DAB converters are analyzed, they satisfy the equation:

$$\begin{cases}V_{g1}=V_{g2}=V_{g3}=\ldots=V_{gNn}\\ i_{o1}=i_{o2}=i_{o3}=\ldots=i_{oNn}\end{cases} \tag{13}$$

The realization of power sharing is to control the output voltage of each DAB converter equal to $V_o/N_n$, where $V_o$ is the total output voltage of the multi-DAB converters. Hence, the control strategy should be expressed with FCS-MPC as:

$$J=\sum_{l=1}^{N_h}(V_{oi}(k+l)-V_o^*)^2 \qquad V_o^*=\frac{V_{ot}}{N_n} \tag{14}$$

From the above three structures and their realizations for power balance, it can be noticed that the power balance is obtained only by controlling the input voltage or output voltage. Hence, the above three conditions can be classified as voltage-controlled power balance.

The next structure remaining to be discussed is the IPOP DAB converters. Similarly, the IPOP DAB converters satisfy that equation as:

$$\begin{cases}V_{g1}=V_{g2}=V_{g3}=\ldots=V_{gNn}\\ V_{o1}=V_{o2}=V_{o3}=\ldots=V_{oNn}\end{cases} \tag{15}$$

Thus, the realization of power sharing is to control the input current or output current of each DAB converter to be balanced. And the output current sharing is considered in this work. To realize output current sharing, the output current of each DAB converter should equal $i_{ot}/N_n$, where $i_{ot}$ is the total output current of the multi-DAB converters. Hence, the control strategy should be expressed with FCS-MPC as:

$$
\begin{aligned}
J &= \sum_{l=1}^{N_h} (i_{oi}(k+l) - i_o^{*})^2 \\
i_o^{*} &= \frac{i_{ot}}{N_n}
\end{aligned} \tag{16}
$$

As seen, IPOP DAB converters can realize the power balance only by controlling the output current. Hence, it is different from the control strategy under the above three conditions.

Although (16) can ensure the current sharing for IPOP DAB converters, it is difficult to be carried out when calculating $i_o(k+1)$. According to the model in (2), it can only predict the output voltage according to the relationship between the capacitor voltage and capacitor current. However, it cannot predict the output current according to this relationship. Hence, (11) can be replaced with the following equation:

$$
\begin{cases}
J = \sum_{l=1}^{N_h} (V_{oi}(k+l) - V_o^{*})^2 \\
V_{oi}(k+1) = V_{oi}(k) + \dfrac{\dfrac{V_{gi}(k)}{2NL}\varphi(k)(1-2\varphi(k)) - \dfrac{P}{N_n V_{oi}(k)}}{C} T_s
\end{cases} \tag{17}
$$

In this way, the power sharing control for DAB converters with four types of connecting structures is realized based on the MPC controllers. Compared with the conventional PI controller, the MPC algorithm can be designed without extra sharing bus or master controllers.

## III. Parameters Estimation based on Kalman Filter

Although MPC is an effective and easy-design algorithm, the drawback of this algorithm is also obvious. The reliance on the system model will influence the robustness of this algorithm as Fig. 3 shows. When the leakage inductance changes, the adjusting time of the system with an updated leakage inductance value will be faster than that without an updated value.

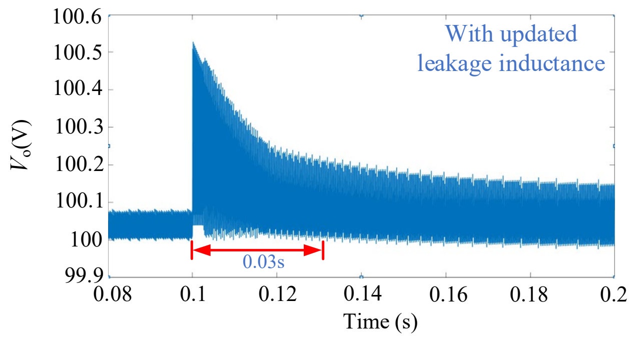


(a)

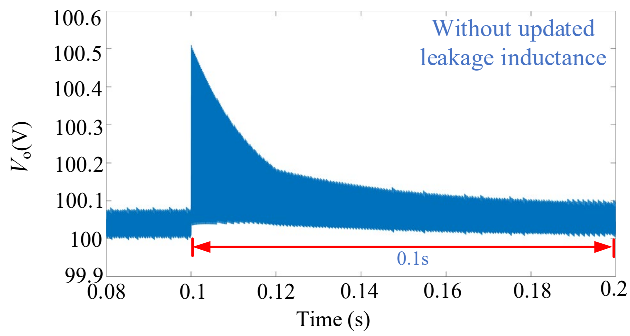


(b)

Fig. 3. Output voltage when leakage inductance changes. (a) With the updated leakage inductance. (b) Without the updated leakage inductance.

In the studied DAB converter, its leakage inductance $L$ is closely tied to the transferred power of the system. When the converter is operating, it cannot be ensured the leakage inductance remains at a constant value. Hence, it is essential to evaluate the value of the inductance and update the latest value to the controller. Besides, the estimation can also provide parameter monitoring for the system. In this paper, a Kalman filter-based estimation method is proposed for evaluating the parameters for the DAB converter. To simplify the calculation, the single DAB converter is considered.

According to the Kalman filter algorithm operating principle and system's parameters, it yields:

$$
\begin{cases}
y(k) = \varphi^{T}{}_{k}\theta_k + v_k \\
\theta_k = \theta_{k-1} + \omega_k
\end{cases} \tag{18}
$$

where $y(k)$ is the output of the system, $\varphi_k$ represents the variables of the system. $v_k$ is the measuring noise. $\theta_k$ is the system's parameters and $\omega_k$ donates the changes in the parameters. Usually, the Kalman filter model in (18) is established based on the system's model. For example, the system's model can be expressed via transferring the $s$ domain transfer function to the $z$ domain as:

$$
G_{vd} = \frac{n_2 z^{-2} + n_1 z^{-1}}{d_2 z^{-2} + d_1 z^{-1} + 1} \tag{19}
$$

Then, the difference equation can be derived as:

$$
y_k + d_2 y_{k-2} + d_1 y_{k-1} = n_2 u_{k-2} + n_1 u_{k-1} \tag{20}
$$

where $u$ is the control variable. Nevertheless, due to the strong non-linear characteristics of the MPC, the system's model cannot be obtained accurately, which will lead to a poor estimation. Hence, the Kalman filter model should be established according to the control principle of the DAB converters based on the MPC. And the estimating process is illustrated as follows.

Define $P(0) = g^{*}I$, where $I$ is an identity matrix and $g$ is a large number. A large $g$ can prevent the system becoming converging at the beginning.

Then the Kalman gain can be defined as:

$$
L_k = P^{+}{}_{k-1}\varphi_k^{T}\left[\varphi_k P^{+}{}_{k-1}\varphi_k^{T} + r_k\right]^{-1} \tag{21}
$$

where $P^{+}{}_{k}$ can be obtained as:

$$
\begin{cases}
P_k = P^{+}{}_{k-1}\left(I - L_k\varphi_k\right) \\
P^{+}{}_{k} = P_k + Q
\end{cases} \tag{22}
$$

Finally, according to the above equation, it yields:

$$
\hat{\theta}_k = \hat{\theta}_{k-1} + L_k[y(k) - \varphi(k)\hat{\theta}_{k-1}] \tag{23}
$$

$\hat{\theta}_k$ donates the estimated parameters from the Kalman filter.

Where $Q$ in (22) donates the covariance matrix, which equals :

$$
\begin{cases}
\hat{\omega}_k = \hat{\theta}_k - \hat{\theta}_{k-1} \\
\hat{Q}_i = [\hat{\omega}_{ik}]^2 \\
Q = diag[[\hat{\omega}_{1k}]^2 \;\; [\hat{\omega}_{2k}]^2 \ldots]
\end{cases} \tag{24}
$$

The elements in $Q$ are decided by the error between each estimated value in the $k$ instant and the estimated value in the $k$-1 instant. Based on this, the Kalman filter for estimating the parameters for the DAB converter can be designed. In this paper, the Klaman filter is designed to estimate both the leakage inductance $L$ and the load $R$.

According to (5) and (18), the variables are replaced according to the DAB converter's model as:

$$\begin{cases} V_o(k+1) = [V_o(k) \quad \frac{V_g(k)T_s[2\varphi(1-\varphi)]}{4}]^T[1-\frac{1}{R(k)C} \quad \frac{1}{L(k)}] + v_k \\ [1-\frac{1}{R(k)C} \quad \frac{1}{L(k)}] = [1-\frac{1}{R(k-1)C} \quad \frac{1}{L(k-1)}] + \omega_k \end{cases} \tag{25}$$

where $R = P/V_o^2$. And the initial value of $g$ is chosen as 10000. The measuring noise $r_k$ is chosen as 0.001.

According to (20), it yields:

$$[1-\frac{1}{R(k)C} \quad \frac{1}{L(k)}]_{es} = [1-\frac{1}{R(k-1)C} \quad \frac{1}{L(k-1)}]_{es} + L(k)[V_o(k+1) - [V_o(k) \quad \frac{V_g(k)T_s[2\varphi(1-\varphi)]}{4}]][1-\frac{1}{R(k-1)C} \quad \frac{1}{L(k-1)}]_{es}] \tag{26}$$

Then, the process of the power sharing MPC algorithm and the parameters estimation method based on the Kalman filter is illustrated as Firstly, the output voltage is sampled, and the phase shifting value is obtained. Then the estimated value of $\theta$, the Kalman gain, and the matrix $P$ are updated. In the next step, the parameters are estimated and then the covariance matrix $Q$ is calculated. Finally, the MPC provides the optimal phase shifting value realizing power sharing control.

## IV. Simulation Results

To validate the proposed power sharing control as well as the estimation method, related simulations are provided based on the system's parameters in Table I.

TABLE I System Parameters.

| Parameters | Symbols | Values |
|---|---|---|
| Input voltage | $V_{in}$ | 400 V |
| Output voltage | $V_o$ | 300 V |
| Leakage Inductance | $L$ | 50 μH 45 μH |
| Capacitor | $C$ | 2000 μF |
| Switching frequency | $f_s$ | 20 kHz |
| Load | $R$ | 50 Ω |
| Transformer Ratio | $N$ | 1:1 |
| *LC* filter inductance | $L_f$ | 200 μH |
| *LC* filter capacitor | $C_f$ | 200 μF |
| Number of DAB converters | $N_n$ | 2 |

Fig. 4 shows the output voltage of DAB 1 and DAB 2 respectively when they are ISOS connected. As seen, the output voltage of each DAB converter equals the desired output voltage of 300 V approximately. Moreover, the difference between these two converters' output voltages is within 1 V, which proves the effectiveness of the power sharing control.

Fig. 5. shows the output voltage of DAB 1 and DAB 2 respectively when they are IPOS connected. As seen, the output voltage of each DAB converter equals the desired output voltage of 300 V approximately. Moreover, the difference between these two converters' output voltages is within 1 V, which proves the realization of the power sharing control.

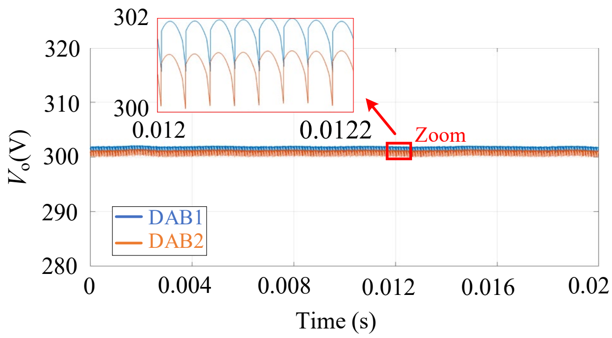


Fig. 4. Output voltage using ISOS structure with leakage inductance $L_1$=50 μH, $L_2$=45 μH.

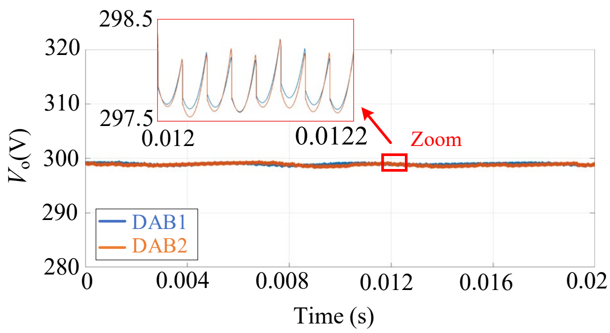


Fig. 5. Output voltage using IPOS structure with leakage inductance $L_1$=50 μH, $L_2$=45 μH.

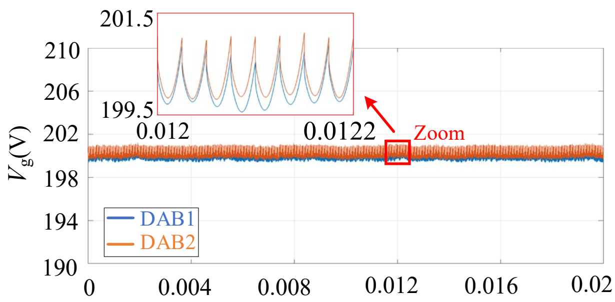


Fig. 6. Input voltage using ISOP structure with leakage inductance $L_1$=50 μH, $L_2$=45 μH.

Fig. 6 shows the input voltage of DAB 1 and DAB 2 respectively when they are ISOP connected. The input voltage of each DAB converter equals half of the total input voltage approximately which is 200 V. Moreover, the difference between these two converters' output voltages is within 0.5 V, which proves the input voltage sharing is realized.

Fig. 7 shows the input voltage of DAB 1 and DAB 2 respectively when they are IPOP connected. From the results, the average output current of each DAB converter equals to 3 A approximately. Moreover, it shows an output current sharing ability within 0.1 A difference. Fig. 8 and Fig. 9 show two outputs of the Kalman filter, which are the first output of 1/$L$ and the second output of 1-1/$RC$. As seen when the leakage inductance changes from 50 μH to 60 μH at 0.005 s, the first output of the Kalman filter can estimate the changing leakage inductance within 0.02 s. When the load changes from 50 Ω to 25 Ω, the second output of the Kalman filter can estimate the changes in load within 0.01 s. And from the comparison in Table II, shows that the estimated error is within 1% and the estimated value is accurate.

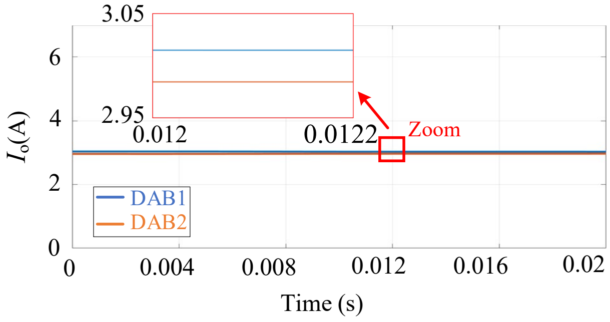


Fig. 7. Average output current using IPOP structure with leakage inductance $L_1$=50 μH, $L_2$=45 μH.

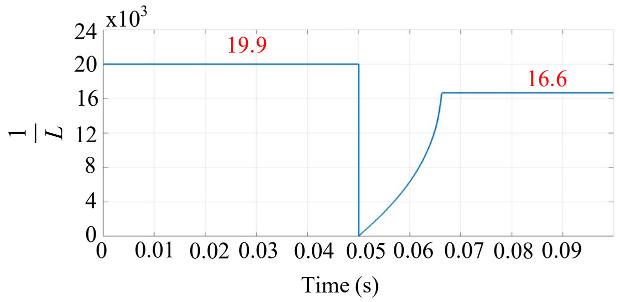


Fig. 8. Kalman filter's first output when leakage inductance $L$ changes at 0.05s from 50 μH to 60 μH.

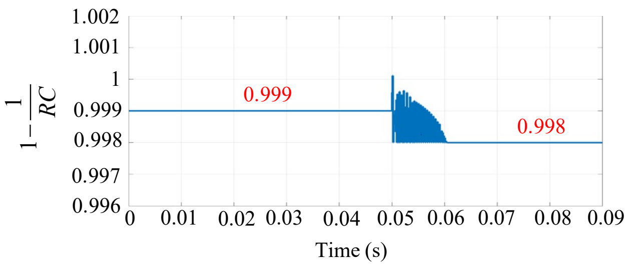


Fig. 9. Kalman filter's second output when load $R$ changes at 0.05s from 50 Ω to 25 Ω.

TABLE II Parameters' Estimation.

| Parameters | Real | Estimated |
|---|---|---|
| $L$ | 50 μH to 60 μH | 50.3 μH to 60.2 μH |
| $R$ | 50 Ω to 25 Ω | 50 Ω to 25 Ω |

## V. Conclusion

This paper proposes a power sharing control for the DAB converters based on the MPC algorithm. By designing the control objective and cost function for the MPC algorithm, power sharing is realized for four different structures of the DAB converters. To guarantee the control robustness, a Kalman filter-based estimation controller is designed for the DAB converter to assess the change of leakage inductance and the load.

In the end, the simulation results provide the validation of the proposed power sharing control. Also, the results prove the effectiveness of the Kalman filter estimation controller when leakage inductance and load change. Based on this, the power sharing and the control performance of the DAB converters can be guaranteed with the proposed method.

## References


[1] T. Dragičević, X. Lu, J. C. Vasquez, et.al, "DC Microgrids—Part I: A Review of Control Strategies and Stabilization Techniques," *IEEE Trans Power Electron.*, vol. 31, no. 7, pp. 4876-4891, July 2016.

[2] S. Sahoo, T. Dragicevic and F. Blaabjerg, "An Event-driven Resilient Control Strategy for DC Microgrids", *IEEE Trans. Power Electron.*, vol. 35, no. 12, pp. 13714-13724, Dec. 2020.

[3] B. Zhao, Q. Song, W. Liu, et.al, "Overview of Dual-active bridge Isolated Bidirectional DC-DC Converter for High-frequency-link Power-conversion System, " *IEEE Trans. Power Electron.*, vol. 29, no. 8, pp. 4091–4106, Aug. 2014.

[4] B. Liu, P. Davari, and F. Blaabjerg, "An Optimized Hybrid Modulation Scheme for Reducing Conduction Losses in Dual Active Bridge Converters", *IEEE J. Emerg. Sel. Top. Power Electron.*, pp. 1-1, Nov. 2019.

[5] X. Zhang, Q.-C. Zhong, andW.-L. Ming, "Stabilization of a cascaded DC converter system via adding a virtual adaptive parallel impedance to the input of the load converter," *IEEE Trans. Power Electron.*, vol. 31, no. 3, pp. 1826–1832, Mar. 2016.

[6] W.-J. Lee and S.-K. Sul, "DC-Link voltage stabilization for reduced DC-Link capacitor inverter," *IEEE Trans. Ind. Appl.*, vol. 50, no. 1, pp. 404–414, Jan. 2014.

[7] T. Dragičević, "Dynamic stabilization of DC microgrids with predictive control of point-of-load converters," *IEEE Trans. Power Electron.*, vol. 33, no. 12, pp. 10872–10884, Dec. 2018.

[8] L. Chen et al., "Predictive Control Based DC Microgrid Stabilization With the Dual Active Bridge Converter," *IEEE Trans. Ind. Electron.*, vol. 67, no. 10, pp. 8944-8956, Oct. 2020.

[9] L. Chen et al., "Moving Discretized Control Set Model-Predictive Control for Dual-Active Bridge With the Triple-Phase Shift," *IEEE Trans. Ind. Electron.*, vol. 35, no. 8, pp. 8624-8637, Aug. 2020.

[10] D. Ma, W. Chen, and X. Ruan, "A Review of Voltage/current Sharing Techniques for Series-parallel-connected Modular Power Conversion Systems", *IEEE Trans. Power Electron.*, vol. 35, no. 11, pp. 12383-12400, 2020.

[11] L. Qu, D. Zhang, and Z. Bao, "Active Output-voltage-sharing Control Scheme for Input Series Output Series Connected DC-DC Converters based on a Master-Slave Structure, " *IEEE Trans. Power Electron.*, vol. 32, no. 8, pp. 6638–6651, Aug. 2017.

[12] M. D. Sha, Z. Guo, T. Luo, et.al, "A General Control Strategy for Input-series-output-series Modular DC-DC Converters, " *IEEE Trans. Power Electron.*, vol. 29, no. 7, pp. 3766–3775, Jul. 2014.

[13] X. Ruan, W. Chen, L. Cheng, C. Tse, H. Yan, and T. Zhang, "Control strategy for Input-series-output-parallel Converters, " *IEEE Trans. Ind. Electron.*, vol. 56, no. 4, pp. 1174–1185, Apr. 2009.

[14] L. Qu, D. Zhang, and Z. Bao, "Output Current-differential Control Scheme for input-series-output-parallel-connected modular dc-dc converters, " *IEEE Trans. Power Electron.*, vol. 32, no. 7, pp. 5699–5711, Jul. 2017.

[15] X. Huang *et al.*, "Large-scale Photovoltaic Generation System Connected to HVDC Grid with Centralized High Voltage and High Power DC/DC converter, " in *Proc. IEEE Int. Conf. Elect. Mach. Syst.*, 2017, pp. 1–6.

[16] K. Siri, K. A. Conner, and C. H. Truong, "Uniform voltage distribution control for paralleled-input, series-output connected converters, " in *Proc. IEEE Aerosp. Conf.*, 2005, pp. 1–11.

[17] Z. Sun, Q. Wang, L. Xiao et.al, "A Simple Sensorless Current Sharing Control for Input-Parallel Output-Parallel Dual Active Bridge Converters," *IEEE Trans. Ind. Electron.*, vol. 69, no. 11, pp. 10819-10833, Nov. 2022.

[18] Y. Panov and M. M. Jovanovic, "Stability and Dynamic Performance of Current-sharing Control for Paralleled Voltage Regulator Modules," *IEEE Trans. Power Electron.*, vol. 17, no. 2, pp. 172-179, March 2002.

[19] F. An, W Song, B. Yu, et.al, "Model Predictive Control with Power Self-balancing of the Output Parallel DAB DC-DC Converters in Power Electronic Traction Transformer", *IEEE J. Emerg. Sel. Top. Power Electron.*, vol. 6, no. 4, pp. 1806-1818, Dec. 2018.

[20] M. Algreer, M. Armstrong, and D. Giaouris, "Active Online System Identification of Switch Mode DC-DC Power Converter based on Efficient Recursive DCD-IIR Adaptive Filter, " *IEEE Trans. Power Electron.*, vol. 27, no. 11, pp. 4425–4435, Nov. 2012.

[21] J. Sun, L. Qiu, X. Liu, et.al, "Modified Model Predictive Control for Three-Phase Dual-Active-Bridge DC-DC Converters with Recursive Least Square Estimation", *IEEE Energy Conversion Congress and Exposition - Asia (ECCE- Asia)*, pp. 720-725, 2021.

[22] M. Ahmeid, M. Armstrong, S. Gadoue, et.al, "Real-time Parameter Estimation of DC-DC converters Using a Self-tuned Kalman Filter", *IEEE Trans. Power Electron.*, vol. 32, pp. 5666-5674, Jul. 2017.